

Optimal Microchannel Planar Reactor as a Switchable Infrared Absorber

Mark E. Alston

ABSTRACT

This paper will propose methods to use leaf vasculature formations to advance a material to act as an infrared block. The research shows the use of microfluidics based flows to direct the structural assembly of a polymer into a thermally functional material. To manage IR radiation stop-band to lower a polymer device phase transition temperature. This paper will determine this functionality by hierarchical multi microchannel network scaling, to regulate laminar flow rate by analysis as a resistor circuit.

Nature uses vasculature formations to modulate irradiance absorption by laminar fluidic flow, for dehydration and autonomous self-healing surfaces as a photoactive system. This paper will focus specifically on pressure drop characterization, as a method of regulating fluidic flow. This approach will ultimately lead to desired morphology, in a functional material to enhance its ability to capture and store energy. The research demonstrates a resistor conduit network can define flow target resistance, that is determined by iterative procedure and validated by CFD. This algorithm approach, which generates multi microchannel optimization, is achieved through pressure equalization in diminishing flow pressure variation. This is functionality significant in achieving a flow parabolic profile, for a fully developed flow rate within conduit networks. Using precise hydrodynamics is the mechanism for thermal material characterization to act as a switchable IR absorber. This absorber uses switching of water flow as a thermal switching medium to regulate heat transport flow. The paper will define a microfluidic network as a resistor to enhance the visible transmission and solar modulation properties by microfluidics for transition temperature decrease.

INTRODUCTION

Microfluidic approach can direct the assembly of a thermally functional material in advancement of energy capture and storage. Using precise hydrodynamic control of a planar microfluidic platform is significant to attain uniform solar radiation adsorption. This characterization in optimal fluidic transport flow is present in natural networks, leaf venation (1,2,3). Leaves use micro capillaries vasculature for the transportation of nutrients, carbon dioxide for photosynthetic mechanisms (4). These fractal structures that are driven by maximizing low dissipation rate for steady state uniform flow, defined by resistance. Hydraulic pressure driven flows can be determined by electrical circuit theory, as a series of resistors in parallel, equal to the sum of total number of channels N (5). Leaves use negative pressure to induce flow that scales linearly in channel networks for fluidic transport that is defined by

hierarchical branch network scaling (6). Each channel (vein succession sequence) is aligned to a specific formation order within a closed loop network (7,8). Microfluidics devices controlled steady state flow within rectangular channel slot geometry will lead to desired material functionality. A thermally functional material by modulating volumetric flow rates of fluid–material interface. This characterization is determined by hierarchical, sequence succession resistance networking. Leaves are examples of this approach, possessing resilient self-healing, mechanical adaptation, and a photoactive system of chemical chain reactions (8). Nature’s nanotechnology will advance materials through biologically inspired engineering. Composite designs are currently hindered by our ability to regulate structural complexity however, nature has developed multifunctional materials based upon adaptive strategies. These nanostructures are founded by reaction interface, achieved by nanoscale ordering aligned to capture and storage of energy in space. This characterization is heat transport regulation across the interface between fluid-material for energy modulation. These properties currently do not apply to translucent materials that are presently energetically weak in visible transmission and offer limited solar energy modulation efficiency. The objective of natural networks is to attain minimum energy output for reduction in pressure drop that is determined by cross section channel geometry and flow rate, Murrays law (11). Microchannels spatial geometry are pressure driven network flows that are proportional to vein density, hierarchy and flow rate (9-14). Using precise hydrodynamic control of a microfluidic platform is governed by fluidic feed in (manifold) channels that can be evaluated as a resistor, figure 1.

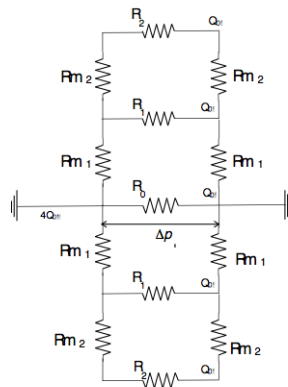


Figure 1. Microfluidic device as a resistor circuit in determining pressure driven flows.

R_m denotes the feed in and extracts manifold resistance and R represents parallel fluidic resistors. ΔP (pressure distribution) is the parameter coefficient that is dependent on current flow and circuit resistance.

THEORY

To evaluate pressure distribution within a planar network, systematic resistance and unifying feed in manifold (R_m) flows is required. Manifolds upstream and downstream channels must reduce flow turbulence in avoidance of unsteady state flows at network node channel branching. This method follows the principles of leaf vein hierarchy of none uniform channel

cross sectional geometry (15,16,17). Each vein has a specific order set within a flow fraction network to reduce pressure drop by fluid flow transportation, in maximizing flow rate (18). This principle was applied to microfluidic flow dependent network to optimize pressure distribution to achieve uniform steady state flows, by theoretical resistance analysis. This was determined in the original microfluidic network device, by sequence of rectangular channel widths succession that was defined as; 2.0,2.3,2.6,2.8 and 3.00mm (19). However this theoretical approach by resistance networking, was determined by a single central microchannel. This resistance seeking targeting worked outwards from the center to define multi microchannel width succession sequencing for tailored flow rates. To test this optimized sequence, manifold upstream and downstream tapered Rm channel resistance was evaluated. An iterative program calculates the width of the tapered manifold at each longitudinal microchannel to influence pressure drop along all channels. Analysis of hydraulic resistance and comparison between the analytical solution and CFD was obtained to assess the widths of the tapered manifold Lm at each longitudinal microchannel y coordinate centreline.

$$Lm_i = y_i - y_{i-1} \quad \text{for } i = 1, 2, 3, 4$$

The widths of the manifold are then given by

$$w_i = w_0 - m.y_i \quad \text{for } i = 0, 1, 2, 3, 4$$

The analysis of resistances determines the average width of each manifold channel:

$$\bar{w}_i = \frac{(w_{i-1} + w_i)}{2} \quad \text{for } i = 1, 2, 3, 4$$

Hydraulic resistance, R , of a longitudinal microchannel has a constant cross-sectional area is given by:

$$R = \frac{\mu Po 2L}{A D_h^2}$$

If we assume that the angle of the manifold taper is small, then the individual flow resistances in the manifold can be calculated using the cross-section at the mid-point.

$$Rm_i = \frac{\mu Po 2Lm_i}{A_i D_{hi}^2} \quad \text{for } i = 1, 2, 3, 4$$

Where A_i and D_{hi} are the area and hydraulic diameter at the mid-point of the manifold Channel

$$A_i = \bar{w}_i h \quad \text{and} \quad D_{hi} = \frac{4A_i}{2(\bar{w}_i + h)} \quad \text{for } i = 1, 2, 3, 4$$

CFD simulations are based on a total flow rate of 9.0 ml/min through the entire device. Half of the device was modeled and therefore a flow rate of 4.5 ml/min = $4.5 \times 10^{-6} / 60 \text{ m}^3/\text{s} = 7.5 \times 10^{-8} \text{ m}^3/\text{s}$ was applied at the inlet manifold port. However, the CFD code needs to use the mass flow rate, \dot{m} , given by;

$$\dot{m} = \rho Q = 997 \times 7.5 \times 10^{-8} = 7.4775 \times 10^{-5} \text{ kg/s}$$

To optimize the design so that the mass flow rate through each channel is

$$\dot{m}_{\text{required}} = \frac{7.4775 \times 10^{-5}}{4.5} \text{ kg/s} = 1.66166 \times 10^{-5} \text{ kg/s}$$

CFD simulation of the initial microchannels widths identified the pressure drops are not optimized due to shortcut pathways through the device. These volumetric flow pathways represents unsteady state flows and will have a direct influence on thermal conductance. This is owing to mass flow rate between upstream and downstream manifolds in the microfluidic network. Mass flow rate in microchannels are defined as $\dot{m}_0, \dot{m}_1, \dots, \dot{m}_4$. CFD indicates unified flow across the microfluidic planar network in the central microchannel is $\sim 21\%$ lower. The flow rates in R_1 to R_4 have a maximum error of 0.4% from the desired mass flow rate. However, the flow rate through the central channel is too small in determining unified parabolic velocity and pressure gradient profile across the microfluidic flow dependent device. Knowing pressure drops (Δp) between upstream and downstream manifolds (R_{m1} to R_{m4}) enables comparisons of theoretical resistance of analytical results through CFD simulation. However an alternative systematic resistance-seeking approach can determine optimization of the microfluidic device as defined by the outermost channel. This would determine and set the resistance target succession iterative procedure by working inwards into the center of the planar device. CFD simulations has already determined present microfluidic device R_4, R_3, R_2 microchannels are close to the optimum uniform distribution of flow. It is the low pressure driven laminar flow of the inner channels R_1 and R_0 that indicate flow rates that are not in agreement with others. The analysis will begin with the known hydraulic resistance R_4 (in this study the outermost channel), and then compute R_3, R_2 , recursively. This is reverse analysis of a central channel, acting as the mechanism to determine resistance seeking. This method of target resistance working inwards in analysis of flow that is a different approach from a leaf fractal like network that is centered on stem vasculature as a central fluidic supply and extract. The advantage of this, the footprint of steady state parabolic laminar flow of the outermost channel width is unknown at the start and the width of the device cannot be known in advance. In this study, a 3mm microchannel, determined the outer-channel edge of the device and the systematic resistance of succession would apply to R_3, R_2, R_1, R_0 . Thus R_4 is known and flow resistances for multi microchannels networking succession can be defined by volumetric flow rate for steady state pressure:

$$Q_1 = Q_2 = Q_3 = Q_4 = Q_0$$

The pressure drop across the outermost longitudinal channel is given by

$$\Delta p_4 = Q_0 R_4$$

Resistance of the other longitudinal channels, R_3

$$\Delta p_3 = Q_0 R_3 = Q_0 R_{m_4} + Q_0 R_4 + Q_0 R_{m_4}$$

$$R_3 = R_{m_4} + R_4 + R_{m_4}$$

$$R_3 = R_4 + 2 R_{m_4}$$

The resistances therefore can be determined recursively using:

$$R_i = R_{i+1} + 2(4-i)R_{m_{i+1}} \quad \text{for } i = 3, 2, 1, 0$$

In the case of N side channels:

$$R_i = R_{i+1} + 2(N - i)Rm_{i+1} \quad \text{for } i = N - 1, \dots, 3, 2, 1, 0$$

The uniform distribution of target resistance succession across the multi microchannels is described by, R ($\text{kg m}^{-4} \text{s}^{-1}$) and determined by the outermost channel, $R(4) = 0.15375808\text{D}+09$. The parallel resistances targeting of this flow dependent network are: $R4 = 0.15375808\text{D}+09$, $R3 = 0.16844248\text{D}+09$, $R2 = 0.18618044\text{D}+09$, $R1 = 0.20512915\text{D}+09$, $R0 = 0.22463418\text{D}+09$.

Each microchannel in this resistance network sequence is to avoid fluids taking the path of least resistance of each channel branching node of upstream supply. The original microfluidic network device, channel widths succession was; 2.0,2.3,2.6,2.8,3.00mm and presented shortcut pathways of varying parallel resistance. The alternative iterative approach corrected succession resistance network for flow rates $Q4 = Q3 = Q2$ and validated CFD. These data results of microfluidic geometry were investigated to determine pressure driven flow rate at; 9.0 and 90.0 ml/min. However at greater flow velocity to achieve uniform distribution flow may be affected by increased turbulence and reduced inertial effects across the planar microfluidic network. CFD analysis of the optimized network using the theoretical resistance succession widths of 3.000, 2.804, 2.613, 2.445 & 2.300mm was investigated table 1.

Table 1. \dot{m} - mass flow generated by CDF simulation for 9.0 and 90.0 ml /min
Total flow rate at 9.0 ml/min

Longitudinal channel i	\dot{m} (kg/s)	Corrected \dot{m} (kg/s)	$\dot{m} / \dot{m}_{\text{required}}$
0	8.21468E-06	1.642936E-05	0.9887
1	1.65499E-05	1.654990E-05	0.9960
2	1.66425E-05	1.664250E-05	1.0016
3	1.66795E-05	1.667950E-05	1.0038
4	1.66885E-05	1.668850E-05	1.0043

Total flow rate at 90.0 ml/min

Longitudinal channel i	\dot{m} (kg/s)	Corrected \dot{m} (kg/s)	$\dot{m} / \dot{m}_{\text{required}}$
0	8.52128E-05	1.704256E-04	1.0256
1	1.64744E-04	1.647440E-04	0.9914
2	1.65677E-04	1.656770E-04	0.9971
3	1.65615E-04	1.656150E-04	0.9967
4	1.66501E-04	1.665010E-04	1.0020

CDF modeling of the device at differing flow rates, 9.0 and 90.0 ml/min was undertaken, figure 2.

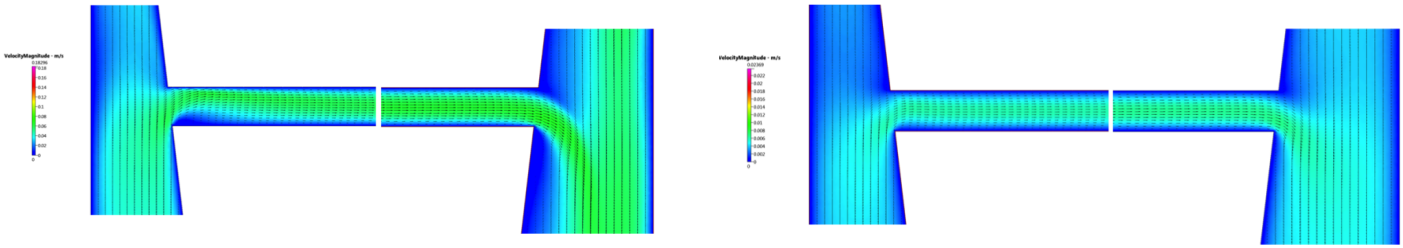


Figure 2. Pressure distributions: Detail of velocity distribution at upstream and downstream of R_3 at a flow rate, (a) 90.0 ml / min, (b) 9.0 ml / min.

The analysis results indicated even at the greater flow rates of 90 ml/min the distribution of the flow between multi microchannel successions remain almost uniform. By setting target systematic resistance enables determination of pressure drop across a planar device for any given flow rate. This enhanced flow fraction network through pressure equalization by diminishing flow pressure variation. However increased flow rate, impacts on uniform thermal conductance across a microfluidic device, for enhanced energy capture. Each microchannel is extracting heat from a material region and this is dependent on fluidic thermal flow.

DISCUSSION

Modulating volumetric flow rates in a device will heighten heat transport across the interface between fluid-material. This ability to lower its phase transition temperature is dependent on an individual microchannel within a networks ability to adsorb, transfer thermal flow across the interface of polymer material layers. Each microchannel is heat seeking, by extraction of thermal energy from a material region. Hierarchical branching resistance network scaling was optimized and validated by CFD. The resistance sequence of an inward working iterative procedure determined a parallel network defined as: 3.000 mm, 2.804 mm, 2.613 mm, 2.445 mm and 2.300 mm. The microfluidic device-sequencing resistance network was analyzed at differing flow rates; 9.0 and 90.0 ml/min and CFD simulation varied the theoretical results. The higher flow rate anticipated results expected high turbulence of unequal distribution of flow across the planar device of increased short cut pathways. These short cut pathways would directly impact on heat flow transport characterization within the microfluidic network configuration. However the 90.0ml/min flow rate distribution almost achieved uniform steady state parabolic flow within this flow dependent network. These results gave validity to the approach of hydraulic resistance knowledge, enables the calculation of pressure drop across a planar device for tailored flow rate, without the need for CFD. When the microfluidic network device was subjected to IR impact 1000 W/m² the device achieved a temperature difference to decrease roughly inversely with flow rate over a pragmatic range of flow. Parabolic velocity flow rate profile of the fluid acted as a constant IR absorber to advance a polymer, to lower its phase

transition temperature. This controlling processing of a functional material of a microfluidic based platform, using extensional flow generated in channels acted as an IR radiation stop band. Each microchannel within the network is a heat seeking absorber by fluid-material interface to regulate material regions as a thermal flow bridge. By modulating volumetric flow rate in the device thermal conductance heat flow was regulated. The 5mm polymer counter plate acted as a partially absorbing 210 W/m² pane by solar radiation impact. The rectangular microchannels of pressure driven laminar flow at, 9.0 ml/min, adsorbed 707 W/m². Heat transport IR transmission temperature through the remaining polymer was 83 W/m². Thermal functionality is determined by the fluid absorber (water 4.18 kJ/l) in smooth flow, without non-linear, turbulence effects. However at greater flow rates within the flow dependent network that achieves uniform pressure gradient, thermal conductance is decreased. This lower material transmission temperature is centered on the fluid (water) thermal properties to absorb IR for heat transport across the planar device. Increased flow rate will reduce the thermal flow capture more strongly due to the combined effects of higher cooling power of the device, the consequence of this is lower IR absorption. Although higher cooling is achieved of the microfluidic device, material phase transmission temperature to act as an IR block is reduced. This part of the experimental laboratory output data indicated the curve at this point is unwanted for solar modulation properties. By modulating volumetric flow rate, we change the temperature increase of the fluid in steady state, as a switchable IR absorber. An increased flow rate gives high transmission temperatures with increased material cooling effects. This functionality offers limited solar-energy modulation and thermal flow transport across the microfluidic platform. In order to evaluate thermal transport flow is depended on fluid-material interface to achieve an energy balance. This energy balance of solar irradiation power absorption is determined by the manipulate position of flow rate for steady state pressure within fictile flow networks.

CONCLUSIONS

Systematic resistance networking of multi microchannels theoretical approach enables uniform planar extensional flow rates through the network for optimized condition. That conclusively demonstrates optimization procedure using precise hydraulic resistance is a valid approach. Such optimization efficiency will advance optically clear composites in energy generation flow design for advanced materials. However a network at higher flow rates, ability to lower its phase transition temperature is diminished. Low volumetric flow rate in steady state enhances solar modulation properties with reduced energy pressure requirement. Energy conservation in flow fraction network is dependent on pressure drop and this has been demonstrated. A dynamic IR absorber, characterization is modulated by temperature-dependence of the absorber in precise laminar flow. This computational design methodology of a microfluidic device in uniform distribution of flow, will direct the assembly of a thermally functional switchable IR absorber for desired functionality.

ACKNOWLEDGMENTS

Science and Technology Facilities Council, U.K for their help and support.

REFERENCES

1. E.Katifori, G.J.Szollosi, M.O.Magnasco, *phys.rev.lett*, **104**,048704 (2010).
2. T.Nelson, N.Dengler, *Plant Cell* . **9**, 1121 (1997).
3. A.M. Turing, The Chemical Basis of Morphogenesis, Philosophical Transaction of the Royal Society of London, Series A, *Biological Science*. **237**, 37-72 (1952).
4. H.Sinoquet. H, G. Sonohat, J. Phattaralerphong. J, C. Godin, *Pant Cell and Environment*, **28** (2005).
5. Oh.W. Kwang, K. Lee, Ahn,Byungwook , E.P.Furlani, *Lab on a Chip*.**12**, 515-545 (2010).
6. L.J.Hickey, *Am, J.Bot.* **60**,17-33 (1973).
7. D. Dengler, J. Kang, *Phys Rev. prl* **104**, 048703 (2010).
8. S.Bohn , M.O.Magnasco, Structure , *Phys. Rev.* **98**, 088702 (2007).
9. R.M.Hubbard, M.G.Ryan, V.Stiller, J.S.Sperry, *Plant. Cell Environ*, **24**, 113-121 (2001).
10. C.D..Murray, *Proc Natl. Acad Sci, U.S.A* .**12**, 207-214 (1926)
11. A.Nardini, M.T.Tyree, F.Pitt , M.A. LoGullo, *Plant Cell Environment*. **23**, 71-79 (2000).
12. A.Nardini, M.T.Tyree , S. Salleo, *Plant Physiol*. **125**, 1700-1709 (2001).
13. N.Wang, F.R.Tan, L.Wan, M.C.Wu, X.M.Zhang, *Biomicrofluidics*. **8**, 054122 (2014).
14. C.K.Boyce, T.J.Brodribb, T.S.Field , M.A.Zwieniecki, *Proc.R.Soc B*. **276**, 1771-1776 (2009).
15. T.J.Brodribb, T.S.Field , G.J.Jordan, *Plant Physil*.**144**, 1890-1898 (2007).
16. S.Salleo, A.Nardini, F.Pitt , M.A. Logullo, *Pant. Cell Environ*. **23**, 71-79 (2000).
17. X.Noblin, L.Mahadevan, I.A. Coomaraswamy, D.A.Weitz, N.M.Holbrook , M.A.Zwienieck, *Proc. Natl. Acad. Sci*. **105**, 9140 – 9144 (2008).
18. Shah,R.K. London,A.I. Laminar flow forced convection in ducts, *Academic press*, ISBN: 0-12-020051-1 (1978).
19. Alston, M. E, Barber, R, *Scientific Reports*. **6**, 31611 (2016).